

## Experimental characterization of a quasi-coherent turbulence structure in the edge plasmas in W7-X

X. Han<sup>1,2</sup>, A. Krämer-Flecken<sup>1</sup>, C. Nührenberg<sup>3</sup>, T. Windisch<sup>3</sup>, G. Fuchert<sup>3</sup>,  
J. Geiger<sup>3</sup>, O. Grulke<sup>3</sup>, S. Liu<sup>1,2</sup>, K. Rahbarnia<sup>3</sup>, and the W7-X team<sup>3</sup>

<sup>1</sup> Forschungszentrum Jülich GmbH, Institut für Energie-und Klimaforschung - Plasmaphysik,  
Partner of the Trilateral Euregio Cluster (TEC), 52425 Jülich, Germany

<sup>2</sup> Institute of Plasma Physics, Chinese Academy of Sciences, 230031 Hefei, People's Republic  
of China

<sup>3</sup> Max-Planck-Institut für Plasmaphysik, 17491 Greifswald, Germany

**Introduction:** Characterizing the nature of turbulence is of importance for understanding the underlying physics of turbulent transport. In the stellarator Wendelstein 7-X (W7-X), the three-dimensional geometry of magnetic fields are designed for a quasi-isodynamic equilibrium at high beta, and the neoclassical transport induced by the bounce-averaged radial drift of trapped particles is strongly reduced. However, the magnetic field strength and the local curvature  $\kappa$  are shifted with respect to each other in both the bean-shaped poloidal and the triangular cross sections of W7-X, that enable us to distinguish between ITGs and TEMs by examining their mode structure. The microinstabilities in W7-X have been predicted to show a significantly reduced growth rates[1].

A poloidal correlation reflectometer (PCR) is designed to investigate the turbulence behaviors at the interface between core and edge plasmas in W7-X, which has been successfully operated during the last two campaigns[2, 3]. In the first W7-X campaign with the limiter configuration, the turbulence rotation and radial electric field are evaluated and compared with the neoclassical calculations. The fluctuation at  $f \approx 18$  kHz has been observed at  $r/a \approx 0.7 - 0.9$  and compared fairly well with the CAS3D simulation[4]. Moreover, an electromagnetic coherent mode at  $f \approx 7$  kHz in the scrape-off layer (SOL) has been observed via both the PCR and the Langmuir probes[5]. The existence of the mode relies on

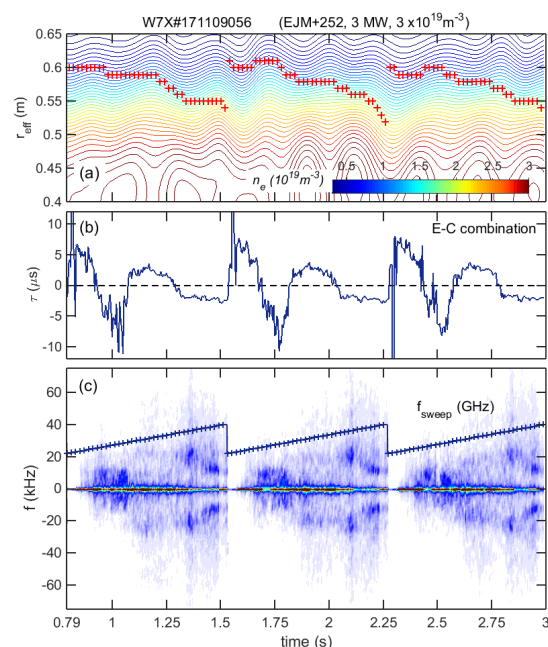


Figure 1: (a) Contour of density profiles. The corresponded cutoff positions of the PCR system are marked as the red crosses. (b) The delay time in the antenna E-C. (c) Cross power spectrum in of E C antennas. The incident frequencies are indicated as the blue crosses.

the heating power, indicating a dependency of the edge profile gradient.

In this paper, a quasi-coherent mode (QCM) in the edge region is studied via measuring the coherency within antenna combinations of PCR. The QCM properties are characterized experimentally and compared with CAS3D simulation. Results indicates that the QCM may contribute to a drift ballooning mode structure.

**Experimental Observations:** Figure 1 shows a typical discharge with the QCM observation in the standard configuration (EJM). In which the ECRH heating power is  $P_{\text{ECRH}} = 3 \text{ MW}$ , and the line-integrated density is  $n_{\text{el}} = 3 \times 10^{19} \text{ m}^{-3}$ . The density profiles in figure 1(a) are measured by the Thomson Scattering (TS) diagnostic, which are interpolated for the time stamps between PCR and TS measurements. The reference ID of 173 is chosen for a standard configuration from the VMEC equilibrium calculation in order to map the data onto the effective minor radius ( $r_{\text{eff}} = a_{\text{LCFS}} \sqrt{\phi}$ ) coordinate. Note that the VMEC-173 is the one with an extended volume in order to include the SOL region. The last-closed flux surface (LCFS) in this configuration is posited at  $a_{\text{eff}} \approx 0.56 \text{ m}$ .

Figure 1(b) shows the delay time ( $\tau$ ) evolution with antenna E and C. The sign in  $\tau$  changes twice within one frequency scan, indicating the probing wave goes through the separatrix of the island and LCFS. In figure 1(c) of the cross power spectrum of E and C antennas, the QCM at  $f \approx 25 \text{ kHz}$  emerges when the cutoff position of the wave locates inside the LCFS. The QCM central frequency decreases to  $f \approx 10 \text{ kHz}$  as the cutoff position moving toward the core. The full width at half maximum in the spectrum is  $\delta f/f \approx 0.25$  at  $f = 25 \text{ kHz}$ . It can be seen in a radial range of  $r_{\text{eff}} \approx 0.56 - 0.53 \text{ m}$ . The QCM is constantly observed in all the three scans in the figure 1(c).

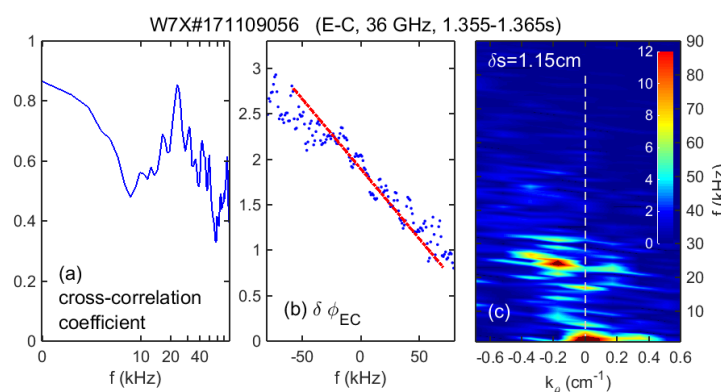


Figure 2: (a) Correlation coefficient calculation from antenna E-C combination. The incident frequency in this time window is  $f = 36 \text{ GHz}$ . (b) Cross-phase calculation in the same time window. (c) frequency-wavenumber spectral density ( $S_{k,f}$ ) in antenna E-C combination in the same time window. The distance in the cutoff layer is  $\delta s = 1.15 \text{ cm}$ , and the negative wavenumber indicates an electron diamagnetic drift direction.

Figure 2 calculates the cross power spectra using antenna E and C at  $f_{\text{PCR}} = 36 \text{ GHz}$ . The central frequency of the QCM is  $f \approx 23 \text{ kHz}$  in figure 2(a). The slope of the cross-phase is linear

in the frequency range of  $f = \pm 100$  kHz in figure 2(b), indicating that dispersive contributions from the turbulence phase velocity can be neglected. The delay time is obtained from the slope of the cross-phase  $\tau = (d\phi/df)/2\pi \approx 2.49 \mu\text{s}$ , which is in consistent with the result in the figure 1(b). The poloidal distance in the corresponded cutoff layer for E and C is  $\delta s \approx 1.15$  cm. Then the wavenumber is obtained  $k_\theta = -0.25 \text{ cm}^{-1}$  propagating in the electron diamagnetic drift direction as shown in figure 2(c).

In general, the poloidal mode number of a turbulence structure is given as  $m = 2\pi f_{\text{mode}}/V_\perp$ , and the wavenumber  $k_\theta = f_{\text{mode}}/V_\perp \rho = m/\rho$ . By neglecting the phase velocity of the turbulence, the perpendicular velocity ( $V_\perp$ ) measured by PCR is equal to the  $E \times B$  velocity. In this discharge,  $V_\perp$  in the edge region inside the LCFS is estimated  $V_\perp = -5 \sim -7$  km/s. The poloidal mode number of the QCM is in the range of  $m = 12 - 20$ , and the wavenumber  $k_\theta \approx 0.2 \sim 0.35 \text{ cm}^{-1}$ . Taking edge electron temperature from TS of  $T_{e,\text{edge}} = 40$  eV into the ion Larmor radius at the sound speed  $\rho_s^2 = c^2 M_i T_e / (e^2 B^2)$ , which leading to the  $k_\theta \rho_s \leq 0.1$ . This result suggests the QCM a drift ballooning mode behavior.

#### Comparison with CAS3D simulation:

A similar ballooning mode structure in the edge region has also been predicted in the CAS3D simulation. Figure 3 illustrates the mode structure in the W7-X low-shear reference case. The line-averaged density is  $n_e = 3 \times 10^{19} \text{ m}^{-3}$  in a  $\text{H}_2$  plasma. The average  $\langle \beta \rangle = 0.02$ , and the pressure profile with a peaking factor of  $\langle \beta_{\text{axis}} \rangle / \langle \beta \rangle = 2$  are taken. The e-folding time is  $\tau_{e,\text{folding}} = 4 \mu\text{s}$ , and the growth rate the mode  $\gamma = 2\pi/\tau_{e,\text{folding}} = 40$  kHz. The mode frequency is higher than the one observed experimentally, it may due to the higher  $\langle \beta \rangle$  taken in the CAS3D simulation.

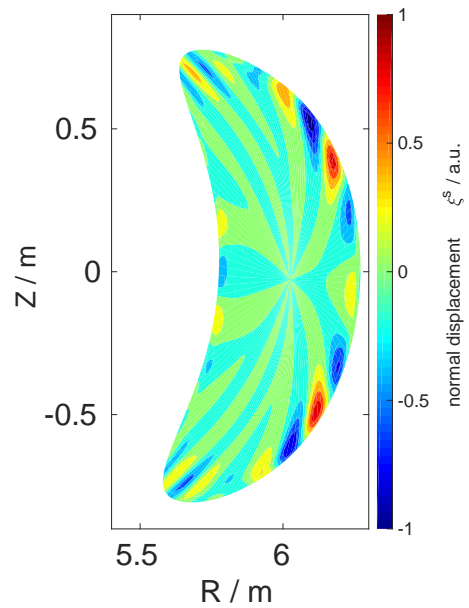


Figure 3: CAS3D simulation.

**Discussion and Conclusion:** Figure 4 summarizes the edge parameters for the QCM observations. The edge density, temperature and pressure are obtained from the last channel inside the LCFS of TS. The decorrelation time ( $\tau_d$ ) is defined as half the width at the  $1/e$  level of the cross-correlation function (CCF) exponential decay. In OP1.2a campaign of W7-X, the edge pressure increases with the increasing of the edge density. The  $\tau_d$  decreases when  $T_{e,\text{edge}}$  rising. The relatively low  $T_{e,\text{edge}}$  level indicates a high electron resistivity and moderately high plasma density. This is considered to drive the instabilities near the edge plasma with relatively high

collision rate. A magnetic fluctuation at  $f \approx 20$  kHz is also observed in the Mirnov coil signal, which shows a steady central frequency with no shift effect. This may be due to a non-localized measurement of Mirnov coils. However, there is no clear correlation shown in the CCF spectrum.

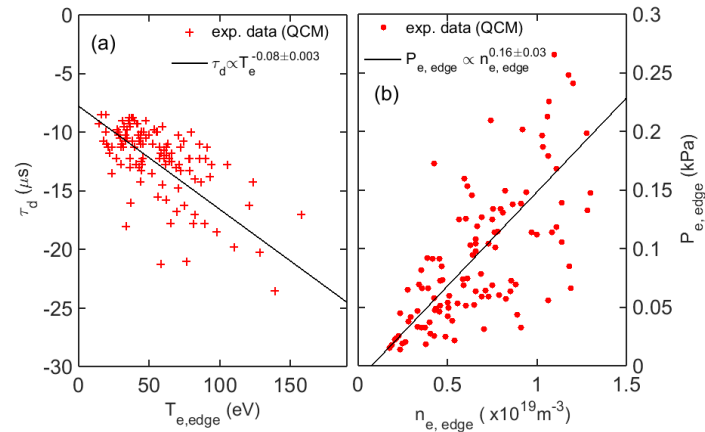


Figure 4: (a) edge pressure dependency of the edge density. (b) decorrelation time  $\tau_d$  dependence of the edge temperature. The black lines are the fitting results.

In conclusion, a QCM in the edge plasma has been studied via the PCR diagnostic in W7-X. The QCM central frequency evolves from  $f = 25$  kHz near the LCFS to  $f = 10$  kHz as the cutoff position moving toward the core. The cross power spectra show a wavenumber of  $k_\theta \approx 0.2 \sim 0.35$ , and the poloidal mode number of the QCM is  $m = 12 - 20$ . The normalized mode size scale is  $k_\theta \rho_s \leq 0.1$ , which is qualitatively consistent with the drift ballooning mode size scale. This QCM structure is also predicted by the CAS3D simulation using a similar plasma parameters. Thus, we tentatively identify the QCM as a drift ballooning mode. However, due to a limited database and diagnostics tools in OP1.2a campaign, the precise instability mechanism and the mode growth rate cannot be determined. This turbulence structure will be studied continuously in the future.

**Acknowledgments** This work has been carried out within the framework of the EUROfusion Consortium and has received funding from the Euratom research and training programme 2014-2018 under grant agreement No 633053, and was supported by the National Natural Science Foundation of China under Grant No. 11605235. The views and opinions expressed herein do not necessarily reflect those of the European Commission.

## References

- [1] J. H. E. Proll, et al., Phys. Plasmas **20** (2013) 122506
- [2] A. Krämer-Flecken, et al., Nucl. Fusion **57** (2017) 066023
- [3] T. Windisch, et al., Plasma Phys. Control. Fusion **59** (2017) 105002
- [4] C. Nührenberg, et al., Nucl. Fusion **56** (2016) 076010
- [5] S. C. Liu, et al., Nucl. Fusion **58** (2018) 046002